Carbon neutral hydrogen storage and release cycles based on dual-functional roles of formamides

Duo Wei [1,2], Xinzhe Shi [1,2], Henrik Junge [2] ✉, Chunyu Du [1] ✉ & Matthias Beller [2] ✉

The development of alternative clean energy carriers is a key challenge for our society. Carbon-based hydrogen storage materials are well-suited to undergo reversible (de)hydrogenation reactions and the development of catalysts for the individual process steps is crucial. In the current state, noble metal-based catalysts still dominate this field. Here, a system for partially reversible and carbon-neutral hydrogen storage and release is reported. It is based on the dual-functional roles of formamides and uses a small molecule Fe-pincer complex as the catalyst, showing good stability and reusability with high productivity. Starting from formamides, quantitative production of CO-free hydrogen is achieved at high selectivity (> 99.9%). This system works at modest temperatures of 90 °C, which can be easily supplied by the waste heat from e.g., proton-exchange membrane fuel cells. Employing such system, we achieve >70% H_2 evolution efficiency and >99% H_2 selectivity in 10 charge-discharge cycles, avoiding undesired carbon emission between cycles.

In the coming decades, society will experience a massive increase in the demand for renewable energy, specifically wind and solar, and to reduce carbon emissions caused by the combustion of fossil fuels[1]. To provide a reliable energy supply and more specifically to meet peak energy demands in densely populated regions as well as to avoid high electricity cost spikes, efficient ways storing fluctuating solar and wind power in both short and long terms are required. Besides classic mechanical approaches to store electric energy, with hydroelectric dams being the most famous ones[2], its conversion to chemical energy is discussed to be a feasible approach[3]. Here, hydrogen which can be easily produced by water electrolysis stands out as a means of an established commercial technology[4,5]. However, handling large quantities of hydrogen is troublesome, since the compressed gaseous and liquid H_2 requires vessels that can withstand high pressures (700 bar) and/or low temperatures (−253 °C) to achieve considerable hydrogen storage capacity. Such methods lead to high energy costs and require specific materials and equipment despite their good H_2 recovery[6]. Alternatively, chemical hydrogen storage-release methods convert H_2 to stable carrier molecules that can be stored and transported at ambient conditions and deliver afterward the stored H_2 on demand via dehydrogenation[7,8]. Such technologies could bridge the production of green H_2 from renewable electricity and its utilization in proton-exchange membrane (PEM) fuel cells to regenerate the stored renewable electricity for terminal energy consumption (Fig. 1a).

Besides the gaseous H_2 carriers e.g., ammonia[9] and methane[10], liquid organic hydrogen carriers (LOHC) offer high reversibility and superior kinetics in (de)hydrogenation, suitable for long distance transport and onboard applications[11,12]. As well-known examples of C1 compounds[13], methane[10], methanol[14], and formic acid (FA)[14,15] have been widely studied concerning hydrogen storage. Compared to ammonia ($\Delta G^0 = +33.3$ kJ mol^{-1}), methane ($\Delta G^0 = +113.6$), and methanol ($\Delta G^0 = +8.9$ kJ mol^{-1}), formic acid (FA) ($\Delta G^0 = -32.9$ kJ mol^{-1}) is more thermodynamically favored in H_2 production process. Therefore, chemical H_2 storage-release cycles applying the H_2/CO_2-FA system have been well-developed in the past decades by using the greenhouse gas CO_2[16,17]. In addition, an intrinsically similar approach including bicarbonate and formate salts has also been investigated in reversible (de)hydrogenation processes ($\Delta G^0 = \pm 0.7$ kJ mol^{-1})[18–20]. Surprisingly,

[1]School of Chemistry and Chemical Engineering, Harbin Institute of Technology, Harbin 150001, P. R. China. [2]Leibniz-Institut für Katalyse e.V, 18059 Rostock, Germany. ✉e-mail: henrik.junge@catalysis.de; cydu@hit.edu.cn; matthias.beller@catalysis.de
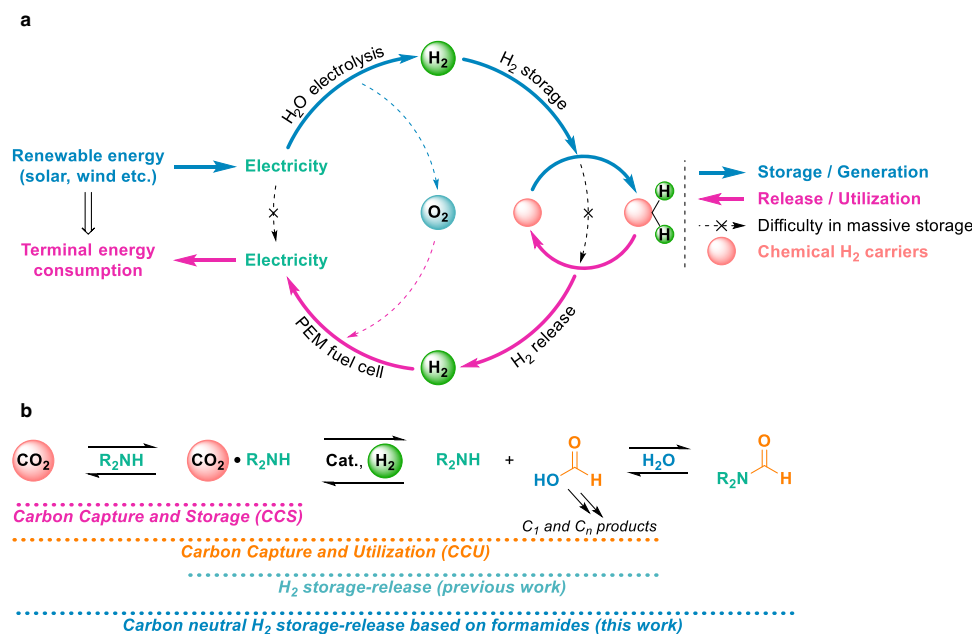
Fig. 1 | Projected sustainable energy utilization based on renewable electricity storage and regeneration bridged by chemical hydrogen storage-release.
a Renewable electricity can be converted to chemical fuel H_2 via water electrolysis. The resulting H_2 is easily transformed into stable chemical H_2 carriers for short- and long-term storage and transportation. The stored H_2 can be released on request to regenerate the renewable electricity in proton-exchange membrane (PEM) fuel cells. **b** Schematic illustration of amine-based carbon capture and storage (CCS), carbon capture and utilization (CCU), previously reported H_2 storage-release, and the strategy of carbon neutral H_2 storage-release based on dual-functional roles of formamides described in this work.

formamides as another class of easily and commercially available C1 compounds derived from CO_2 reduction in the presence of amines have been rarely studied directly in H_2 storage-release cycles[21–23].

It's worth noting that as CO_2 capturing reagents amines are frequently used in carbon capture and storage (CCS) processes[24], and further utilization of the CO_2-amine adducts (captured CO_2) in subsequent hydrogenation allows to produce renewable fuels and chemicals, so called carbon capture and utilization (CCU)[25]. As one of the most prominent examples of CCU, the "George Olah Methanol Plant" in Iceland is based on local renewable energy and CO_2[26]. Its total electrical energy demand and the overall efficiency reach 9.5 MWh/t methanol and 60%. Notably, such CCU processes also provide feasible approaches for sustainable chemical H_2 storage-release applications based on interconversion of CO_2 and C1 compounds (e.g., FA; Fig. 1b)[8]. For example, recently our group developed a reversible H_2 storage-release method based on amino acid lysine promoted CO_2 capture and its reversible hydrogenation to FA[17]. On the other hand, FA in the presence of amines could be easily dehydrated to formamides[27] which combine the carbon capturing reagent amines with the H_2 storage material FA. Therefore, the direct use of formamides as H_2 carriers is practically desired due to their dual-functional roles: the structurally incorporated FA is responsible for H_2 storage-release, and the built-in amines provide a carbon capture and utilization (CCU) strategy leading to an ultimate carbon neutral H_2 storage-release system (Fig. 1b). Compared to the hydrogen contents of FA (4.34 wt%), the ones of various formamides (1.50–3.17 wt%) are slightly lower but still higher than that of common formate salts (1.02–2.85 wt%, Fig. 2a). Bearing in mind that equivalent CO_2 is emitted together with H_2 in FA dehydrogenation process which generally requires a post carbon capturing process to reduce carbon emissions[14], in addition, H_2 storage using formate produces bicarbonate salts which could be decomposed to CO_2 as frequently reported[20]. Besides, another H_2 storage technology using H_2 storage alloys, e.g. magnesium hydrides[28], generally represent hydrogen contents of 1–6 wt%. However, their inferior (de)hydrogenation kinetics, life cycle, and harsh operation conditions (up to 500 °C) make them currently not suitable for most of the applications[28,29].

So far, expensive noble metal-based catalysts still dominate the area of H_2 storage and release. Therefore, the search of suitable non-noble metal catalysts and their efficient utilization in reversible H_2 storage-release cycles are particularly important. As a class of versatile catalysts, iron-based pincer complexes[14,30–42] have been studied respectively in hydrogenation[43–48] and dehydrogenation[49–51], attracting many interests for potentially reversible H_2 storage-release applications[37,38,52–54]. Owing to the metal-ligand cooperation effect, tridentate pincer complexes with a nitrogen donor (N-H) offer effective and stable catalysis in both hydrogenation and dehydrogenation steps[55–57]. As representatives, iron pincer complexes are used in CO_2 hydrogenation to produce FA (or its formate salts)[58–62], formamides[27], and methanol[63], as well as the H_2 production from FA[64–72] and methanol[73]. To the best of our knowledge, no single iron catalyst has been reported for combined H_2 storage and H_2 release cycles yet. On the basis of our interest in developing efficient methodologies for H_2 storage and utilization by using non-noble metal catalysts, we describe herein a concept of iron promoted partially reversible carbon neutral H_2 storage-release cycles in a single device based on dual-functional roles of formamides.

Results and discussion
Concept of reversible carbon neutral hydrogen storage-release cycles based on dual-functional roles of formamides
The concept of iron catalyzed reversible carbon neutral hydrogen storage-release cycles based on dual-functional roles of formamides is illustrated in Fig. 2b. Following the hydrogen release pathway (indicated in pink color), formamide (F_1) is firstly hydrolyzed into formic acid (FA) and corresponding amine (A_1), afterward FA participates in the catalytic cycles of dehydrogenation and hydrogenation. Here the mild potentials of (de)hydrogeantion are provided by redox active iron complexes containing non-innocent pincer ligands[62,64]. It's worth noting that CO_2 by-product is captured in situ and stored in the presence of amine (A_1) initially liberated from formamide hydrolysis. Even though the individual steps of formamides hydrolysis, FA (or formates) dehydrogenation and their reverse reactions are known, the presented hydrogen storage-release concept enables the reuse of in situ captured

CO_2, which allows to (1) retain the hydrogen storage material CO_2 in the reaction, therefore, maintain the theoretical hydrogen storage capacity in successive H_2 storage-release cycles, (2) avoid undesired carbon release during dehydrogenation processes, and (3) provide superior H_2 selectivity/purity compared to other H_2 carrier systems. Following the hydrogen storage pathway (indicated in blue color), the stored CO_2 can be re-hydrogenated to FA which is then (partially) converted to formamide (F_1) via dehydration condensation with corresponding amine (A_1). Thanks to the dual-functional roles of formamides, the built-in amine (A_1) is beneficial to both H_2 storage and H_2 release processes by acting as CO_2 absorbent, providing a carbon capture and utilization (CCU) strategy to ensure the H_2 storage capacity and carbon neutrality of the overall H_2 storage-release process.

Following the concept vide supra, both formamide hydrolysis as well as formamide formation were investigated. Thus, initially the hydrolysis process was performed under alkaline conditions[74,75] and a proportional relationship between the base (KOH) loading and FA yields was found (Figs. S1–2). Accordingly, equimolar ratio of base to formamide is necessary to provide a sufficient amount of H_2 carrier for the subsequent H_2 storage-release cycles. Afterwards, the reaction between different amines and FA to produce formamides was examined (Figs. S3–4)[27]. Interestingly, in this latter condensation process piperazine (A_3) gave a much better yield of the corresponding formamides (22%) compared to morpholine (A_1, 1%) and piperidine (A_2, 1%) under typical reaction conditions used for catalysis (90 °C, 12 h). Obviously, using longer reaction time (72 h) and higher temperature (140 °C) allows to increase the amount of formamide products (A_1 47%, A_2 14%, A_3 46%). Overall, the hydrolysis of formamides to FA and amines is more favored under alkaline condition, than its reverse dehydration condensation.

Next, the CO_2 capture effect of those amines was also investigated (Figs. S5-7). Under CO_2 pressure (2 bar, 30 min.), both bicarbonate and carbamate species of the corresponding amines were obtained as products in the following order: piperidine (A_2, 69%), piperazine (A_3, 55%), and morpholine (A_1, 42%). These results can be well explained by the reported pKa values of the three amines: A_2 (11.22) > A_3 (9.73) > A_1 (8.36)[76,77]. Under direct air capture conditions (air flow 1.8 L min^{-1}, ca. 400 ppm CO_2, 36 h), piperazine (A_3) led to the highest yield of the corresponding carbamate species (32%) compared to piperidine (A_2, 15%) and morpholine (A_1, 8%). This is attributed to the stronger hydrogen bonding in piperazine (A_3) compared to the other two amines[78]. After all, these results demonstrate the good carbon capture ability of amines A_1, A_2, and A_3, especially with CO_2 concentration at ppm level.
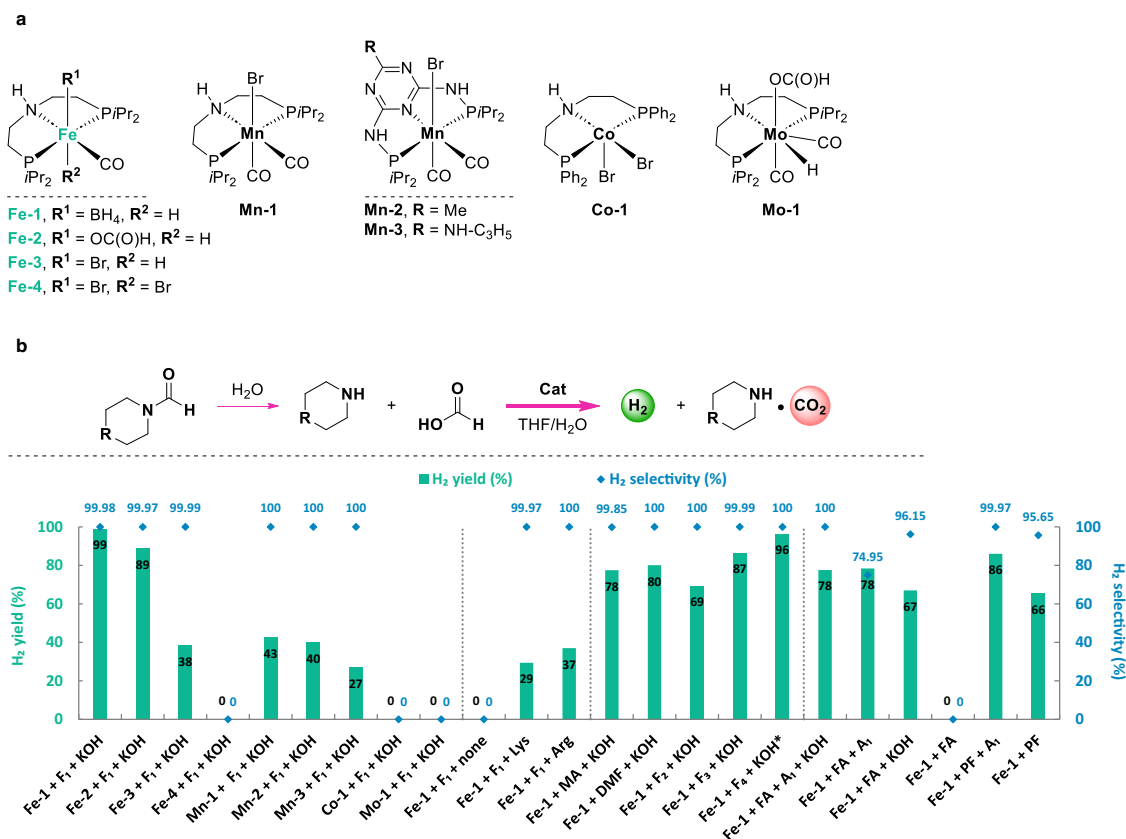
Catalytic hydrogen production based on formamides

Representative non-noble metal pincer complexes (Fig. 3a) were utilized as catalysts in hydrogen production process starting from formamides and the results are summarized in Fig. 3b. Iron pincer-complexes **Fe-1** and **Fe-2**, which were used in formic acid dehydrogenation[64], led to the best yields of H_2 99% and 89% (Figs. S8–9), respectively. Other tested catalysts based on Mn, Co and Mo gave significantly lower H_2 yields (up to 43%). In the absence of external base, no H_2 was produced. Drastically decreased H_2 yields (29% and 37%) were observed after changing the base from KOH to amino acids lysine (Lys) and arginine (Arg), which were recently disclosed for reversible H_2 storage-release involving CO_2 hydrogenation[17]. Indeed, utilizing stoichiometric amounts of Lys or Arg gave only trace amount of FA due to slower formamide (F_1) hydrolysis (1–2% yields, Fig. S2). For hydrogen production also the nature of formamides was examined. Notably, inexpensive and industrially available simple formamides i.e., methanamide (MA) and dimethylformamide (DMF) gave also good H_2 yields (78% and 80%, respectively). However, due to practical considerations, e.g. ammonia and dimethylamine are highly
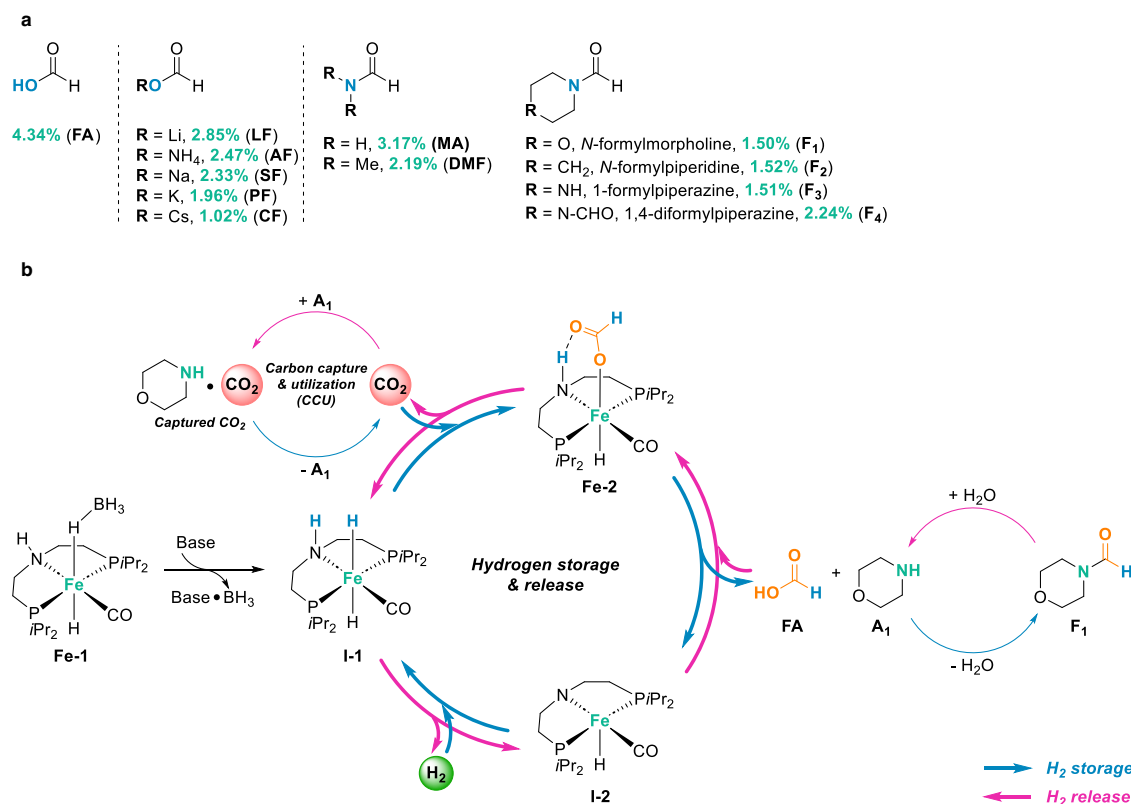
Fig. 2 | Concept of reversible carbon neutral hydrogen storage-release cycles based on dual-functional roles of formamides. a Hydrogen content of formic acid and its derivatives (wt%, indicated in green color). **b** Schematic illustration of the concept of pincer-type iron complex catalyzed reversible carbon neutral H_2 storage and release based on dual-functional roles of formamides.

Fig. 3 | Catalytic hydrogen production from formamides. a Non-noble metal-based pincer complexes utilized in this study. **b** Comparison of activity under various conditions towards catalytic hydrogen production. Standard conditions: N-formylmorpholine (F_1, 10 mmol), KOH (10 mmol), catalyst (5 μmol, 500 pm), THF/ H_2O (5/5 mL), 90 °C, 16 h. *1,4-Diformylpiperazine (F_4, 5.0 mmol) was used. Yields are based on formyl group in formamides. The dotted lines serve as guides to the eye.

volatile and difficult to handle, we utilized their heavier congeners. As the best candidates, N-formylmorpholine (F_1) and 1,4-diformylpiper-azine (F_4) led to quantitative yields of H_2, while N-formylpiperidine (F_2) and 1-formylpiperazine (F_3) gave 69% and 87% H_2 yields, respectively.

The base (KOH) loading in catalytic dehydrogenation process was then investigated: in the presence of 25, 50, 75 mol% of KOH, partial H_2 yields (37-61%) and lower H_2 selectivity were observed (Fig. S10). In the absence of KOH, no conversion of formamide (F_1) occurred as indicated by NMR monitoring on the reaction mixture (Fig. S11). Lewis acids are known to assist dehydrogenation processes catalyzed by iron pincer catalysts[64]. However, inferior H_2 yield (85%) and selectivity (92.5%) were observed in the presence of 10 mol% $LiBF_4$ compared to the standard conditions (Figs. S10 and S34). Changing THF to other organic solvents, i.e., 2-methyl THF (2-MTHF), ethanol, triglyme, 1,4-dioxane, and DMSO, H_2 were observed in 47-74% yields. Using water as sole solvent or under neat conditions, no hydrogen was found due to the low solubility of the catalyst. Decreased H_2 yield (87%) was observed by lowering the reaction temperature to 80 °C, while elevated temperature (100 °C) did not promote the reaction but resulted in increased CO concentration (14 ppm; Fig. S41). In all other cases using **Fe-1** complex and formamides, CO was not detected by gas chromatography (below the CO quantification limit of 10 ppm).

### Comparison on different hydrogen carrier systems in catalytic hydrogen production

Under the optimal conditions, the here presented system utilizing formamides is superior regarding both the H_2 productivity and selectivity compared to other H_2 carriers i.e., formic acid (FA) and potassium formate (PF; Fig. 3b). Specifically, replacing formamide F_1 with FA

and amine A_1, decreased H_2 yields (78%) were observed with H_2 selectivity of 100% (in the presence of KOH) and 74.9% (in the absence of KOH). Notably, 80 ppm CO were detected in the H_2 storage system of FA and A_1 (Fig. S27). Loading FA with KOH, further decreased H_2 yield (67%) was observed, while in the presence of FA only, no dehydrogenation occurred. On the other hand, starting from potassium formate (PF), H_2 was obtained in yields of 86% (in the presence of A_1) and 66% (in the absence of A_1).

Catalytic hydrogen storage in formates and formamides

Next, the process of H_2 storage in formates and formamides was investigated by using hydrogenation of CO_2 or potassium bicarbonate in the presence of amines as model reactions (Fig. 4a)[27,62,79]. In general, the hydrogenation of CO_2 or potassium bicarbonate in the presence of morpholine (A_1), piperidine (A_2), and piperazine (A_3) gave good total yields of formates and formamides (82–100%). Specifically, morpholine (A_1) and piperidine (A_2) led to comparable results regarding the yields of formates (90-97%) and formamides (2–6%), while piperazine (A_3) resulted in a significantly higher amount of formamide product (31%) using CO_2 as carbon source (Fig. 4b, left side, Figs. S50-52). It's worth noting that the amine promoted CO_2 capture product carbamate was formed as minor species in bicarbonate hydrogenation reaction (Fig. S51), thereby avoiding the release of free carbon dioxide even under basic conditions.

Afterwards, variation of reaction parameters in the hydrogenation step using bicarbonate was performed in the presence of morpholine (A_1, Fig. 4b, right side, Fig. S53). Reducing the H_2 pressure from 60 bar stepwise to 40, 20, and 10 bar, total yields of formates and formamides decreased from 99 to 43%. Moreover, lowering the reaction
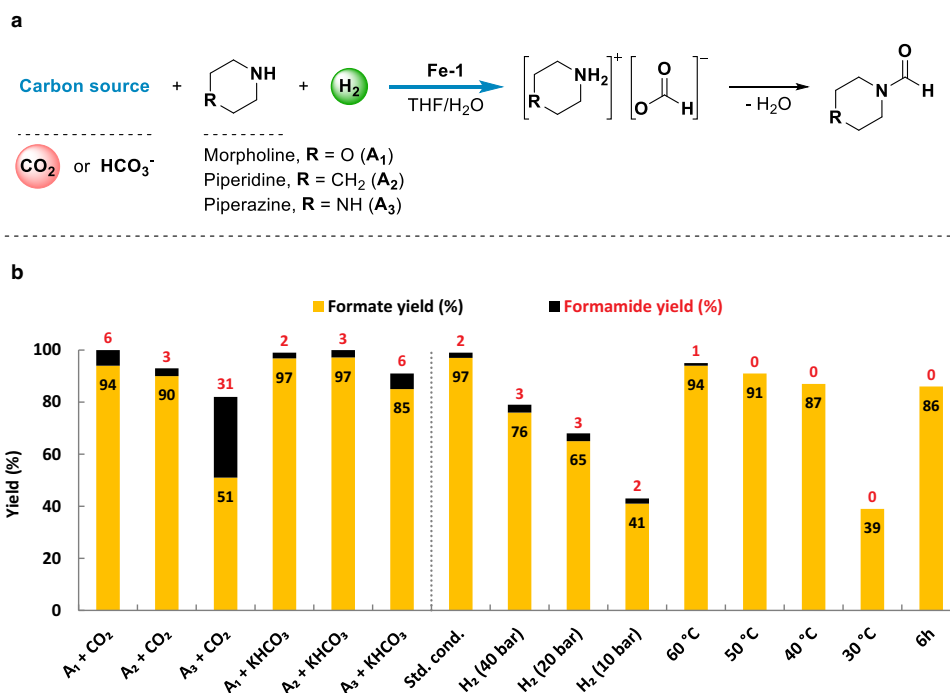
Fig. 4 | Catalytic hydrogen storage in formates and formamides. a Catalytic hydrogen storage process via hydrogenation of CO_2 or potassium bicarbonate in the presence of amines. **b** Left side: comparison of activity towards hydrogen storage with different amines (A_1, A_2, and A_3) and carbon sources (CO_2 and $KHCO_3$). Standard conditions: amine (10 mmol), CO_2 (20 bar) or $KHCO_3$ (10 mmol), **Fe-1** (5 μmol, 500 ppm), H_2 (60 bar), THF/H_2O (5/5 mL), 90 °C, 12 h. Right side: variation of reaction parameters in hydrogenation of $KHCO_3$ with morpholine. Standard conditions: morpholine (A_1, 10 mmol), $KHCO_3$ (10 mmol), **Fe-1** (5 μmol, 500 ppm), H_2 (60 bar), THF/H_2O (5/5 mL), 90 °C, 12 h. Yields are based on amine. The dotted lines serve as guides to the eye.

temperature from 90 °C to 60, 50, and 40 °C, no obvious loss of hydrogen storage capacity was observed, while further decrease to 30 °C, drastically dropped the formate yield to 39%. Further, time dependent product generation of hydrogen storage and release reactions catalyzed by **Fe-1** was investigated (Table S1). Lower total yields of formates and formamides were obtained in 3 and 6 h (66% and 87%, respectively) in hydrogenation reactions with morpholine (A_1) and CO_2. On the other hand, performing the dehydrogenation reactions with *N*-formylmorpholine (F_1) in shorter reaction times led to decreased H_2 yields (29% in 4 h and 49% in 8 h). These results demonstrate that long reaction times are indeed required.

Promoting effect of amines in hydrogen storage and release processes

Next, we explored the promoting effect of seven additional amines in formate dehydrogenation and bicarbonate hydrogenation in more detail (Fig. 5). In addition to A_1, A_2, and A_3, classical amines which are widely utilized in CO_2 hydrogenation and corresponding dehydrogenation processes were tested (Fig. 5a). In hydrogen production reactions (Fig. 5b), the presence of amines A_1, A_2, and A_3 gave high H_2 yields (up to 92%) and selectivity (up to 100%) compared to the one without amine (56% yield and 95% selectivity). Trials with other amines i.e., diazabicycloundecene (DBU)[52,80,81], diazabicyclooctane (DABCO), trihexylamine (THA)[81], and dimethyloctylamine (DMOA)[82,83] resulted in moderate H_2 yields (55% to 76%). However, no H_2 was produced by using tetramethylguanidine (TMG). Interestingly, the two basic amino acids Lys and Arg led to H_2 in 87% and 90% yields, respectively[17,20,84].

In the corresponding hydrogen storage process (Fig. 5c, Fig. S54), amines A_1, A_2, and A_3 gave quantitative yields of formates and formamides[27], while 64% of formate were obtained in the absence of amine. Moreover, DBU, DABCO[85], THA, DMOA, Lys, and Arg led to either lower formate yields (23% to 87%) or even inhibited amide formation. On the other hand, TMG gave nearly quantitative yields of formate and formamide even though it was not active in the H_2

production process at all[85]. As there is no obvious direct correlation of pKa of the applied amine and the storage capacity there will be other factors that potentially influence the system, i.e., solubility and boiling point of amines, hydrogen bonding, steric hindrance, catalyst poisoning etc. After considering the H_2 productivity and selectivity in dehydrogenation (Fig. 5b) and total yields of formates and formamides in hydrogenation (Fig. 5c), we concluded that morpholine (A_1) and piperazine (A_3) are the most suitable amine promoters among all other tested amines. Although formate generation dominates at milder conditions (90 °C, 12 h), formamide yields could be improved at higher temperature and longer reaction time (140 °C, 72 h; Fig. S3), therewith formally clothing the formamide-based hydrogen storage cycle. However, due to practicability milder conditions were employed in subsequent catalytic (de)hydrogenation reactions, as this also allows for efficient and partially reversible H_2 storage (Fig. 5b, c).

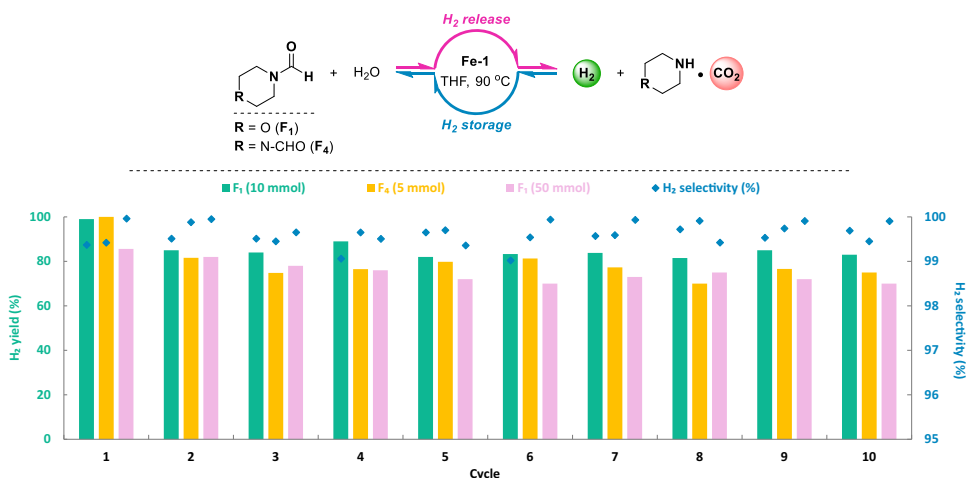### Carbon neutral hydrogen storage-release cycles based on dual-functional roles of formamides

After having optimized conditions in hand for both elementary steps, (a) H_2 release from formamides and (b) corresponding H_2 storage process, we turned our attention to the combination of these hydrogenation and dehydrogenation processes in a single device. The overall "carbon neutral" hydrogen cycle was performed in a closed autoclave starting by dehydrogenation of commercially available formamides using the well-designed catalyst **Fe-1** (500 ppm) in the presence of KOH in aqueous THF solution (90 °C, 16 h). Afterwards, the reactor was cooled to room temperature (r.t., 25 °C) and the generated hydrogen was released carefully to the manual burettes and analyzed by GC. Then, the reactor was charged with H_2 (60 bar) and heated to 90 °C without changing the reaction mixture (H_2 storage step). After the hydrogen uptake stopped (12 h), the overpressure of H_2 was released at r.t. and the autoclave was subjected once more to the H_2 release step (90 °C, 16 h). Following this procedure, 10 H_2 storage-release cycles were performed over 20 days (Fig. 6, Figs. S55−63). Notably, during the
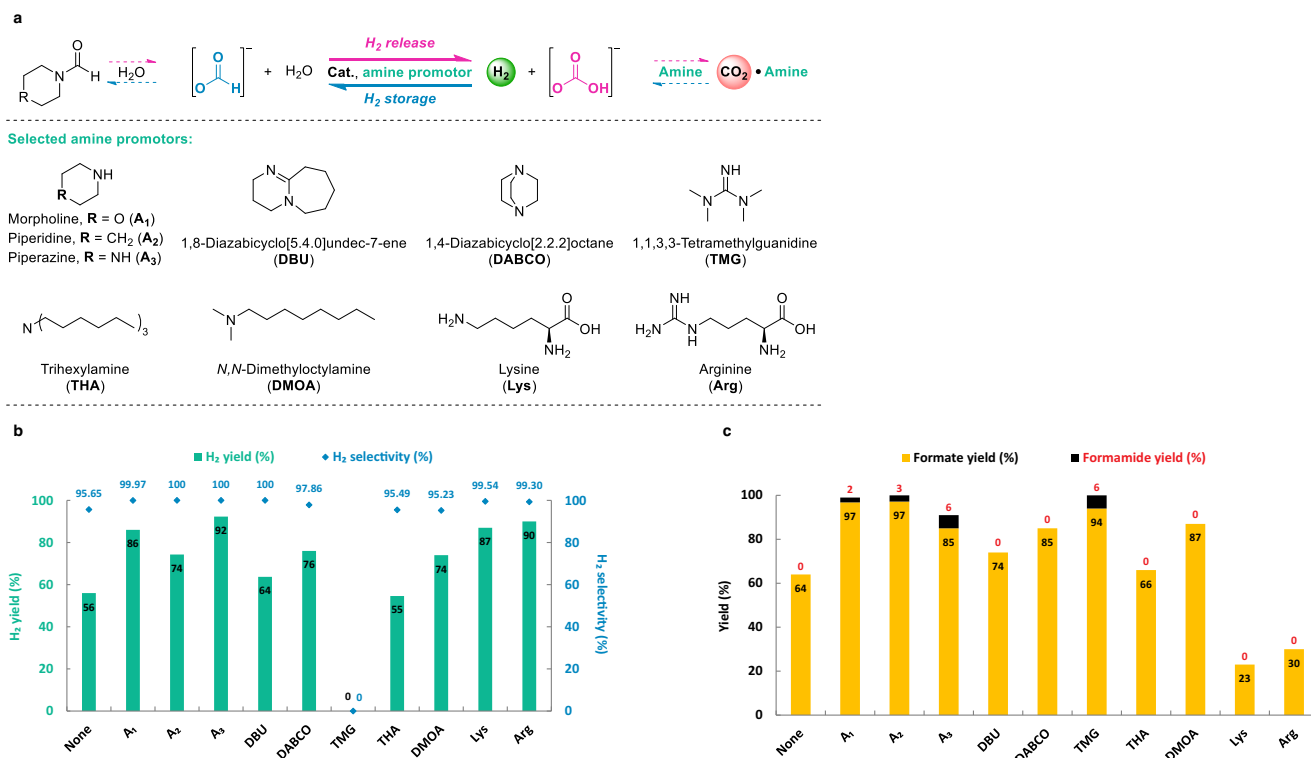
Fig. 5 | Comparison between selected amine promotors in hydrogen storage and release reactions. a Chemical structures of selected amine promotors utilized in formate dehydrogenation and bicarbonate hydrogenation. **b** Hydrogen production from formate in the presence of various amines. Standard conditions: KHCO$_2$ (10 mmol), amine (10 mmol), **Fe-1** (5 µmol), THF/H$_2$O (5/5 mL), 90 °C, 16 h.

Yields are based on KHCO$_2$. **c** Hydrogenation of bicarbonate in the presence of various amines. Standard conditions: KHCO$_3$ (10 mmol), amine (10 mmol), **Fe-1** (5 µmol, 500 ppm), THF/H$_2$O (5/5 mL), H$_2$ (60 bar), 90 °C, 12 h. Yields are based on KHCO$_3$.

Fig. 6 | Fe promoted partially reversible carbon neutral hydrogen storage-release cycles using formamides. Hydrogen evolution in the storage-release cycles applying formamides. Standard conditions: formamide, KOH (1.0 equiv.),

Fe-1 (500 ppm), THF/H$_2$O (5/5 mL), 90 °C. The cycles started from dehydrogenation (16 h), then hydrogenation (12 h, 60 bar of H$_2$) was performed. Yields are based on formyl group in formamides.

whole time, only H$_2$ is charged and discharged and the reloading of hydrogen storage material, catalyst, solvents, additives is not necessary. Even though the iron pincer complexes are generally sensitive to air (oxygen), once the H$_2$ storage-release cycles are in operation, the whole system is closed and generally under over-pressure of H$_2$. On the other hand, air has also to be excluded from the system in order to suppress the hydrogen-air explosions (4.0–75.6%v/v of H$_2$ in air).

^{31}P NMR spectra of pre- and post-reaction samples (after 1 cycle) revealed that the original signal of **Fe-1** complex (99.6 ppm) was

shifted to lower field (114.0 ppm) after the catalytic dehydrogenation reaction (Fig. S64). This signal is assigned to iron pincer derivative **I-2** (Fig. 2) and considered as the resting state in (de)hydrogenation reactions[64]. Besides, only minor species were found in the spectra which might either be the stereoisomers (e.g., trans- and cis-configurations) of the iron pincer complexes or their decomposition products[86].

Comparing the different tested formamides, 1,4-diformylpiperazine (F$_4$) resulted in higher H$_2$ selectivity (>99.5%) than N-

formylmorpholine (F_1, >99.0%) at 10 mmol loading due to the better carbon capture ability of the corresponding amine piperazine (A_3) compared to morpholine (A_1) especially at low CO_2 concentration (Fig. S5). Slightly lower H_2 yields were observed with F_4 (>70%) compared to F_1 (>82%) over 10 H_2 charge-discharge cycles, due to the lower hydrogen storage capacity using corresponding amines A_3 than A_1 (Fig. 4b). To our delight, upscaling reactions applying *N*-formylmorpholine (F_1, 50 mmol) reached 86% H_2 yield in the first cycle, even though gradually decreased yields were observed at 70% in the 10th cycle. Overall, H_2 can be obtained in more than 70% yield and 99% selectivity in 10 charge-discharge cycles (Table S2). For a direct application of the generated hydrogen in PEM fuel cells and to avoid the poisoning of platinum electrodes[87], it is important to note that CO was not detected (below the GC quantification limit of 10 ppm) in the H_2 stream. Advantageously, both the hydrogenation and dehydrogenation steps operated at a temperature level of 90 °C, which can be supplied by the waste heat from e.g., PEM fuel cells or hydrogen internal combustion engines[88].

In conclusion, we demonstrate partially reversible hydrogen storage-release cycles utilizing formamides. This class of hydrogen storage materials has been largely overlooked despite their attractive physical and chemical properties (inertness, hydrogen content, toxicity, boiling point, etc.). In the presented system, the inherent components of formamides play a dual-functional roles: (a) the formic acid part enables H_2 storage and release and (b) the built-in amines provide a carbon capture and utilization (CCU) strategy allowing for an overall "carbon neutral" energy storage system. By using well-designed iron catalyzed hydrogenation and dehydrogenation steps, selective hydrogen formation (CO below detection limit of GC) under mild conditions and high catalyst productivity as well as stability (>20 days) were achieved. To the best of our knowledge, this is also one of the rare examples that an iron based catalytic system allows multiple H_2 storage-release cycles in a single device.

Starting from carbon dioxide or bicarbonate in the presence of selected amines, H_2 storage proceeded with quantitative total yields of formamides and formates at comparably low temperature (<100 °C). Among the different tested amines, morpholine (A_1) and piperazine (A_3) exhibited superior behavior in both H_2 storage and H_2 release processes. The feasibility of combined hydrogenation and dehydrogenation processes in a single device was demonstrated in 10 H_2 charge-discharge cycles catalyzed by an iron complex under mild reaction conditions. Advantageously, the presented system is partially reversible and no reloading of hydrogen storage material, catalyst, solvents, additives is necessary during the whole process.

Methods

Calculation of the hydrogen contents (wt%)
The hydrogen contents (wt%) of formic acid, formate salts, and formamides are calculated as follows:

$$\text{wt\%}_{\text{formic acid}} = M_{H2}/(M_{\text{formic acid}}) \times 100\% \tag{1}$$

$$\text{wt\%}_{\text{formate salt}} = M_{H2}/(M_{\text{formate salt}} + M_{H2O}) \times 100\% \tag{2}$$

$$\text{wt\%}_{\text{formamide}} = (M_{H2} \times N)/(M_{\text{formamide}} + M_{H2O} \times N) \times 100\% \tag{3}$$

where M is the molecular weight, N is the number of formyl groups per formamide molecule.

Standard procedure for catalytic dehydrogenation starting from formamides
Under an argon atmosphere, *N*-formylmorpholine (F_1, 1 mL, 10 mmol), base (10 mmol), catalyst (5 μmol), THF (5 mL) and H_2O (5 mL) were added to a 100 mL autoclave equipped with a magnetic stir bar. Then, the reaction mixture was heated and stirred in a pre-heated oil bath for 16 h. The reactor was cooled to r.t. (25 °C) and the inside pressure was released carefully to the manual burettes. A 5 mL degassed syringe was used to obtain a gas sample analyzed by gas chromatography (GC, CO quantification limit of 10 ppm). Yield of H_2 is calculated as follows:

$$\text{Yield}_{H2} = (\text{mmol } H_2)/(\text{mmol formyl group in formamides}) \times 100\% \tag{4}$$

Standard procedure for catalytic hydrogenation of CO_2 or bicarbonate
Under an argon atmosphere, amine (10 mmol), CO_2 (20 bar) or $KHCO_3$ (1 g, 10 mmol), **Fe-1** (2 mg, 5 μmol), THF (5 mL) and H_2O (5 mL) were added to a 100 mL autoclave equipped with a magnetic stir bar. After pressurizing the reactor with H_2 (60 bar), the reaction mixture was heated and stirred on a pre-heated oil bath for 12 h. Then, the reactor was cooled to r.t. (25 °C) and the overpressure was carefully released. A biphasic reaction mixture was obtained containing a transparent organic upper layer and an aqueous yellow lower layer. Addition of deionized water (ca. 3 mL) to the above mentioned biphasic mixture resulted in a homogeneous solution[17]. Imidazole (170 mg, 2.5 mmol) was added as an NMR internal standard (I.S.) to the reaction mixture, which was then analyzed by ^{1}H NMR with ca. 0.1 mL D_2O to lock the signals. Yields of formate and formamide are calculated as follows:

$$\text{Yield}_{\text{formate}} = (\text{mmol formate})/(\text{mmol amine}) \times 100\% \tag{5}$$

$$\text{Yield}_{\text{formamide}} (\text{mmol formamide})/(\text{mmol amine}) \times 100\% \tag{6}$$

Standard procedure for catalytic H_2 evolution in the H_2 storage-release cycles
The H_2 storage-release cycles start from the dehydrogenation (H_2 release): **Fe-1** (2 mg, 5 μmol, 500 ppm), *N*-formylmorpholine (F_1, 1 mL, 10 mmol), KOH (561 mg, 10 mmol), THF (5 mL) and H_2O (5 mL) were added to a 100 mL autoclave equipped with a magnetic stir bar. The reaction mixture was then heated and stirred in a pre-heated oil bath at 90 °C for 16 h. The reactor was cooled to r.t. (25 °C) and the stored hydrogen was released carefully to the manual burettes then the content of the gas phase was analyzed with a 5 mL degassed syringe by gas chromatography (GC, CO quantification limit of 10 ppm). The autoclave was then filled with 60 bar of H_2, heated and stirred on a pre-heated oil bath at 90 °C for 12 h (H_2 storage). After the completion of H_2 storage, the reactor was cooled to r.t. (25 °C) and the overpressure was carefully released. Then the autoclave was subjected to the H_2 release step once again. Following such process, the H_2 evolution in the H_2 storage-release cycles were implemented over 20 days. Yield of H_2 is calculated according to Eq. (4).

Data availability
All data generated or analyzed during this study are included in the published article and its supplementary information files. Data are also available from the Corresponding Author upon request.

References
1. Anaba, S. A. & Olubusoye, O. E. In *Affordable and Clean Energy* (eds W. L. Filho et al.) 1–13 (Springer, 2020).
2. Stocks, M., Stocks, R., Lu, B., Cheng, C. & Blakers, A. Global atlas of closed-loop pumped hydro energy storage. *Joule* **5**, 270–284 (2021).
3. Schiffer, Z. J. & Manthiram, K. Electrification and decarbonization of the chemical industry. *Joule* **1**, 10–14 (2017).

4. Yan, Z., Hitt, J. L., Turner, J. A. & Mallouk, T. E. Renewable electricity storage using electrolysis. *Proc. Natl. Acad. Sci. USA* **117**, 12558–12563 (2020).

5. Mac Dowell, N. et al. The hydrogen economy: A pragmatic path forward. *Joule* **5**, 2524–2529 (2021).

6. Wei, D. et al. Toward a hydrogen economy: Development of heterogeneous catalysts for chemical hydrogen storage and release reactions. *ACS Energy Lett.* **7**, 3734–3752 (2022).

7. Forberg, D. et al. Single-catalyst high-weight% hydrogen storage in an *N*-heterocycle synthesized from lignin hydrogenolysis products and ammonia. *Nat. Commun.* **7**, 13201 (2016).

8. Wei, D., Sang, R., Moazezbarabadi, A., Junge, H. & Beller, M. Homogeneous carbon capture and catalytic hydrogenation: Toward a chemical hydrogen battery system. *JACS Au* **2**, 1020–1031 (2022).

9. Chatterjee, S., Parsapur, R. K. & Huang, K.-W. Limitations of ammonia as a hydrogen energy carrier for the transportation sector. *ACS Energy Lett.* **6**, 4390–4394 (2021).

10. Fan, W. K. & Tahir, M. Recent trends in developments of active metals and heterogenous materials for catalytic CO_2 hydrogenation to renewable methane: A review. *J. Environ. Chem. Eng.* **9**, 105460 (2021).

11. Zhu, Q.-L. & Xu, Q. Liquid organic and inorganic chemical hydrides for high-capacity hydrogen storage. *Energy Environ. Sci.* **8**, 478–512 (2015).

12. Preuster, P., Papp, C. & Wasserscheid, P. Liquid organic hydrogen carriers (LOHCs): Toward a hydrogen-free hydrogen economy. *Acc. Chem. Res.* **50**, 74–85 (2017).

13. Mesters, C. A selection of recent advances in C1 chemistry. *Annu. Rev. Chem. Biomol. Eng.* **7**, 223–238 (2016).

14. Sordakis, K. et al. Homogeneous catalysis for sustainable hydrogen storage in formic acid and alcohols. *Chem. Rev.* **118**, 372–433 (2018).

15. Eppinger, J. & Huang, K.-W. Formic acid as a hydrogen energy carrier. *ACS Energy Lett.* **2**, 188–195 (2017).

16. Schwarz, F. M., Moon, J., Oswald, F. & Müller, V. Biological hydrogen storage and release through multiple cycles of bi-directional hydrogenation of CO_2 to formic acid in a single process unit. *Joule* **6**, 1304–1319 (2022).

17. Wei, D., Sang, R., Sponholz, P., Junge, H. & Beller, M. Reversible hydrogenation of carbon dioxide to formic acid using a Mn-pincer complex in the presence of lysine. *Nat. Energy* **7**, 438–447 (2022).

18. Grubel, K., Jeong, H., Yoon, C. W. & Autrey, T. Challenges and opportunities for using formate to store, transport, and use hydrogen. *J. Energy Chem.* **41**, 216–224 (2020).

19. Bahuguna, A. & Sasson, Y. Formate-bicarbonate cycle as a vehicle for hydrogen and energy storage. *ChemSusChem* **14**, 1258–1283 (2021).

20. Wei, D., Shi, X., Sponholz, P., Junge, H. & Beller, M. Manganese promoted (Bi)carbonate hydrogenation and formate dehydrogenation: Toward a circular carbon and hydrogen economy. *ACS Cent. Sci.* **8**, 1457–1463 (2022).

21. Kothandaraman, J. et al. Efficient reversible hydrogen carrier system based on amine reforming of methanol. *J. Am. Chem. Soc.* **139**, 2549–2552 (2017).

22. Shao, Z. et al. Reversible interconversion between methanol-diamine and diamide for hydrogen storage based on manganese catalyzed (de)hydrogenation. *Nat. Commun.* **11**, 591 (2020).

23. Xie, Y., Hu, P., Ben-David, Y. & Milstein, D. A reversible liquid organic hydrogen carrier system based on methanol-ethylenediamine and ethylene urea. *Angew. Chem. Int. Ed.* **58**, 5105–5109 (2019).

24. Bui, M. et al. Carbon capture and storage (CCS): the way forward. *Energy Environ. Sci.* **11**, 1062–1176 (2018).

25. Cuéllar-Franca, R. M. & Azapagic, A. Carbon capture, storage and utilisation technologies: A critical analysis and comparison of their life cycle environmental impacts. *J. CO2 Util.* **9**, 82–102 (2015).

26. Olah, G. A., Mathew, T., Goeppert, A. & Surya Prakash, G. K. Difference and significance of regenerative versus renewable carbon fuels and products. *Top. Catal.* **61**, 522–529 (2018).

27. Jayarathne, U., Hazari, N. & Bernskoetter, W. H. Selective iron-catalyzed *N*-formylation of amines using dihydrogen and carbon dioxide. *ACS Catal.* **8**, 1338–1345 (2018).

28. Ouyang, L. et al. Magnesium-based hydrogen storage compounds: A review. *J. Alloys Compd.* **832**, 154865 (2020).

29. Zhao, D.-L. & Zhang, Y.-H. Research progress in Mg-based hydrogen storage alloys. *Rare Met.* **33**, 499–510 (2014).

30. Zell, T. & Milstein, D. Hydrogenation and dehydrogenation iron pincer catalysts capable of metal–ligand cooperation by aromatization/dearomatization. *Acc. Chem. Res.* **48**, 1979–1994 (2015).

31. Gorgas, N. & Kirchner, K. Isoelectronic manganese and iron hydrogenation/dehydrogenation catalysts: Similarities and divergences. *Acc. Chem. Res.* **51**, 1558–1569 (2018).

32. Jones, W. D. in *Organometallics* for *Green Catalysis* (eds P. H. Dixneuf & J-F Soulé) 141–174 (Springer International Publishing, 2019).

33. Bauer, G. & Hu, X. Recent developments of iron pincer complexes for catalytic applications. *Inorg. Chem. Front.* **3**, 741–765 (2016).

34. Werkmeister, S., Neumann, J., Junge, K. & Beller, M. Pincer-type complexes for catalytic (De)hydrogenation and transfer (De)hydrogenation reactions: recent progress. *Chem. Eur. J.* **21**, 12226–12250 (2015).

35. Wang, W.-H., Himeda, Y., Muckerman, J. T., Manbeck, G. F. & Fujita, E. CO_2 hydrogenation to formate and methanol as an alternative to photo- and electrochemical CO_2 reduction. *Chem. Rev.* **115**, 12936–12973 (2015).

36. Bernskoetter, W. H. & Hazari, N. in *Pincer Compounds* (ed D. Morales-Morales) 111–131 (Elsevier, 2018).

37. Bernskoetter, W. H. & Hazari, N. Reversible hydrogenation of carbon dioxide to formic acid and methanol: Lewis acid enhancement of base metal catalysts. *Acc. Chem. Res.* **50**, 1049–1058 (2017).

38. Zell, T. & Langer, R. Iron-catalyzed hydrogenation and dehydrogenation reactions with relevance to reversible hydrogen storage applications. *Recycl. Catal.* **2**, 87–109 (2015).

39. Alig, L., Fritz, M. & Schneider, S. First-row transition metal (De)hydrogenation catalysis based on functional pincer ligands. *Chem. Rev.* **119**, 2681–2751 (2019).

40. Li, H., Gonçalves, T. P., Lupp, D. & Huang, K.-W. PN3(P)-pincer complexes: Cooperative catalysis and beyond. *ACS Catal.* **9**, 1619–1629 (2019).

41. Filonenko, G. A., van Putten, R., Hensen, E. J. M. & Pidko, E. A. Catalytic (de)hydrogenation promoted by non-precious metals – Co, Fe and Mn: recent advances in an emerging field. *Chem. Soc. Rev.* **47**, 1459–1483 (2018).

42. Chen, X. & Yang, X. Mechanistic insights and computational design of transition-metal catalysts for hydrogenation and dehydrogenation reactions. *Chem. Rec.* **16**, 2364–2378 (2016).

43. Chakraborty, S., Bhattacharya, P., Dai, H. & Guan, H. Nickel and iron pincer complexes as catalysts for the reduction of carbonyl compounds. *Acc. Chem. Res.* **48**, 1995–2003 (2015).

44. Bhattacharya, P. & Guan, H. Synthesis and catalytic applications of iron pincer complexes. *Comments Inorg. Chem.* **32**, 88–112 (2011).

45. Glüer, A. & Schneider, S. Iron catalyzed hydrogenation and electrochemical reduction of CO_2: The role of functional ligands. *J. Organomet. Chem.* **861**, 159–173 (2018).

46. Zell, T. & Langer, R. From ruthenium to iron and manganese—A mechanistic view on challenges and design principles of base-metal hydrogenation catalysts. *ChemCatChem* **10**, 1930–1940 (2018).

47. Dai, H., Li, W., Krause, J. A. & Guan, H. Experimental evidence of syn H–N–Fe–H configurational requirement for iron-based bifunctional hydrogenation catalysts. *Inorg. Chem.* **60**, 6521–6535 (2021).

48. Jiao, H., Junge, K., Alberico, E. & Beller, M. A comparative computationally study about the defined m(II) pincer hydrogenation catalysts (m = fe, ru, os). *J. Comput. Chem.* **37**, 168–176 (2016).

49. Zell, T. & Langer, R. CO_2-based hydrogen storage – formic acid dehydrogenation. *Phys. Sci. Rev* **3**, 20170012 (2018).

50. Onishi, N., Kanega, R., Kawanami, H. & Himeda, Y. Recent progress in homogeneous catalytic dehydrogenation of formic acid. *Molecules* **27**, 455 (2022).

51. Balaraman, E., Nandakumar, A., Jaiswal, G. & Sahoo, M. K. Iron-catalyzed dehydrogenation reactions and their applications in sustainable energy and catalysis. *Catal. Sci. Technol.* **7**, 3177–3195 (2017).

52. Curley, J. B., Smith, N. E., Bernskoetter, W. H., Hazari, N. & Mercado, B. Q. Catalytic formic acid dehydrogenation and CO_2 hydrogenation using iron PNRP pincer complexes with isonitrile ligands. *Organometallics* **37**, 3846–3853 (2018).

53. Chakraborty, S. et al. Well-defined iron catalysts for the acceptorless reversible dehydrogenation-hydrogenation of alcohols and ketones. *ACS Catal.* **4**, 3994–4003 (2014).

54. Chakraborty, S., Brennessel, W. W. & Jones, W. D. A molecular iron catalyst for the acceptorless dehydrogenation and hydrogenation of *N*-heterocycles. *J. Am. Chem. Soc.* **136**, 8564–8567 (2014).

55. Khusnutdinova, J. R. & Milstein, D. Metal–ligand cooperation. *Angew. Chem. Int. Ed.* **54**, 12236–12273 (2015).

56. Wodrich, M. D. & Hu, X. Natural inspirations for metal–ligand cooperative catalysis. *Nat. Rev. Chem.* **2**, 0099 (2017).

57. Stevens, M. A. & Colebatch, A. L. Cooperative approaches in catalytic hydrogenation and dehydrogenation. *Chem. Soc. Rev.* **51**, 1881–1898 (2022).

58. Smith, N. E., Bernskoetter, W. H., Hazari, N. & Mercado, B. Q. Synthesis and catalytic activity of PNP-supported iron complexes with ancillary isonitrile ligands. *Organometallics* **36**, 3995–4004 (2017).

59. Langer, R. et al. Low-pressure hydrogenation of carbon dioxide catalyzed by an iron pincer complex exhibiting noble metal activity. *Angew. Chem. Int. Ed.* **50**, 9948–9952 (2011).

60. Rivada-Wheelaghan, O., Dauth, A., Leitus, G., Diskin-Posner, Y. & Milstein, D. Synthesis and reactivity of iron complexes with a new pyrazine-based pincer ligand, and application in catalytic low-pressure hydrogenation of carbon dioxide. *Inorg. Chem.* **54**, 4526–4538 (2015).

61. Bertini, F. et al. Efficient and mild carbon dioxide hydrogenation to formate catalyzed by Fe(II) hydrido carbonyl complexes bearing 2,6-(diaminopyridyl)diphosphine pincer ligands. *ACS Catal.* **6**, 2889–2893 (2016).

62. Zhang, Y. et al. Iron catalyzed CO_2 hydrogenation to formate enhanced by Lewis acid co-catalysts. *Chem. Sci.* **6**, 4291–4299 (2015).

63. Lane, E. M., Zhang, Y., Hazari, N. & Bernskoetter, W. H. Sequential hydrogenation of CO_2 to methanol using a pincer iron catalyst. *Organometallics* **38**, 3084–3091 (2019).

64. Bielinski, E. A. et al. Lewis acid-assisted formic acid dehydrogenation using a pincer-supported iron catalyst. *J. Am. Chem. Soc.* **136**, 10234–10237 (2014).

65. Mellone, I. et al. Selective formic acid dehydrogenation catalyzed by Fe-PNP pincer complexes based on the 2,6-diaminopyridine scaffold. *Organometallics* **35**, 3344–3349 (2016).

66. Zell, T., Butschke, B., Ben-David, Y. & Milstein, D. Efficient hydrogen liberation from formic acid catalyzed by a well-defined iron pincer complex under mild conditions. *Chem. Eur. J.* **19**, 8068–8072 (2013).

67. Curley, J. B., Bernskoetter, W. H. & Hazari, N. Additive-free formic acid dehydrogenation using a pincer-supported iron catalyst. *ChemCatChem* **12**, 1934–1938 (2020).

68. Curley, J. B., Townsend, T. M., Bernskoetter, W. H., Hazari, N. & Mercado, B. Q. Iron, cobalt, and nickel complexes supported by a iPrPNPhP pincer ligand. *Organometallics* **41**, 301–312 (2022).

69. Guan, C., Pan, Y., Zhang, T., Ajitha, M. J. & Huang, K.-W. An update on formic acid dehydrogenation by homogeneous catalysis. *Chem. Asian J.* **15**, 937–946 (2020).

70. Iglesias, M. & Fernández-Alvarez, F. J. Advances in nonprecious metal homogeneously catalyzed formic acid dehydrogenation. *Catalysts* **11**, 1288 (2021).

71. Younas, M., Rezakazemi, M., Arbab, M. S., Shah, J. & Rehman, W. U. Green hydrogen storage and delivery: Utilizing highly active homogeneous and heterogeneous catalysts for formic acid dehydrogenation. *Int. J. Hydrog. Energy* **47**, 11694–11724 (2022).

72. Mellmann, D., Sponholz, P., Junge, H. & Beller, M. Formic acid as a hydrogen storage material—development of homogeneous catalysts for selective hydrogen release. *Chem. Soc. Rev.* **45**, 3954–3988 (2016).

73. Alberico, E. et al. Selective hydrogen production from methanol with a defined iron pincer catalyst under mild conditions. *Angew. Chem. Int. Ed.* **52**, 14162–14166 (2013).

74. Blumberger, J., Ensing, B. & Klein, M. L. Formamide hydrolysis in alkaline aqueous solution: insight from ab initio metadynamics calculations. *Angew. Chem. Int. Ed.* **45**, 2893–2897 (2006).

75. Slebocka-Tilk, H., Sauriol, F., Monette, M. & Brown, R. S. Aspects of the hydrolysis of formamide: revisitation of the water reaction and determination of the solvent deuterium kinetic isotope effect in base. *Can. J. Chem.* **80**, 1343–1350 (2002).

76. Hall, H. K. Jr. Correlation of the base strengths of amines[1]. *J. Am. Chem. Soc.* **79**, 5441–5444 (1957).

77. Khalili, F., Henni, A. & East, A. L. L. pKa values of some piperazines at (298, 303, 313, and 323) K. *J. Chem. Eng. Data* **54**, 2914–2917 (2009).

78. Parkin, A., Oswald, I. D. H. & Parsons, S. Structures of piperazine, piperidine and morpholine. *Acta Cryst* **B60**, 219–227 (2004).

79. Kar, S., Goeppert, A., Kothandaraman, J. & Prakash, G. K. S. Manganese-catalyzed sequential hydrogenation of CO_2 to methanol via formamide. *ACS Catal.* **7**, 6347–6351 (2017).

80. Hsu, S.-F. et al. A rechargeable hydrogen battery based on Ru catalysis. *Angew. Chem. Int. Ed.* **53**, 7074–7078 (2014).

81. Filonenko, G. A., Van Putten, R., Schulpen, E. N., Hensen, E. J. M. & Pidko, E. A. Highly efficient reversible hydrogenation of carbon dioxide to formates using a ruthenium PNP-pincer catalyst. *ChemCatChem* **6**, 1526–1530 (2014).

82. Enthaler, S. et al. Exploring the reactivity of Nickel pincer complexes in the decomposition of formic acid to CO_2/H_2 and the hydrogenation of $NaHCO_3$ to HCOONa. *ChemCatChem* **7**, 65–69 (2015).

83. Mellone, I., Bertini, F., Peruzzini, M. & Gonsalvi, L. An active, stable and recyclable Ru(ii) tetraphosphine-based catalytic system for hydrogen production by selective formic acid dehydrogenation. *Catal. Sci. Technol.* **6**, 6504–6512 (2016).

84. Wei, D., Junge, H. & Beller, M. An amino acid based system for CO_2 capture and catalytic utilization to produce formates. *Chem. Sci.* **12**, 6020–6024 (2021).

85. Kothandaraman, J., Goeppert, A., Czaun, M., Olah, G. A. & Prakash, G. K. S. CO_2 capture by amines in aqueous media and its subsequent conversion to formate with reusable ruthenium and iron catalysts. *Green Chem.* **18**, 5831–5838 (2016).

86. Curley, J. B. et al. Understanding the reactivity and decomposition of a highly active iron pincer catalyst for hydrogenation and dehydrogenation reactions. *ACS Catal.* **11**, 10631–10646 (2021).

87. Alayoglu, S., Nilekar, A. U., Mavrikakis, M. & Eichhorn, B. Ru–Pt core–shell nanoparticles for preferential oxidation of carbon monoxide in hydrogen. *Nat. Mater.* **7**, 333–338 (2008).

88. Wilberforce, T. et al. Recovery of waste heat from proton exchange membrane fuel cells—A review. *Int. J. Hydrog. Energy*, in press, https://doi.org/10.1016/j.ijhydene.2022.08.069, (2022).

Author contributions

Conceptualization, D.W. and X.S.; Methodology, D.W. and X.S.; Investigation, D.W. and X.S.; Resources, H.J. and M.B; Writing, D.W., X.S., H.J., C.D., and M.B.; Funding Acquisition, H.J., C.D., and M.B.; Supervision, D.W., H.J., C.D., and M.B. All authors have read and agreed to the published version of this work.

Competing interests

The authors declare no competing interests.

Additional information

Supplementary information The online version contains supplementary material available at https://doi.org/10.1038/s41467-023-39309-4.

Correspondence and requests for materials should be addressed to Henrik Junge, Chunyu Du or Matthias Beller.

Reprints and permissions information is available at http://www.nature.com/reprints

Publisher's note Springer Nature remains neutral with regard to jurisdictional claims in published maps and institutional affiliations.